Virologica Sinica 39 (2024) 301–308

Contents lists available at ScienceDirect

Virologica Sinica

journal homepage: www.keaipublishing.com/en/journals/virologica-sinica
www.virosin.org

Research Article

Identification of fangchinoline as a broad-spectrum enterovirus inhibitor through reporter virus based high-content screening

Qiu-Yan Zhang [a,b,1], Jia-Qi Li [b,1], Qi Li [b], Yang Zhang [c], Zhe-Rui Zhang [b], Xiao-Dan Li [d], Hong-Qing Zhang [b], Cheng-Lin Deng [b], Feng-Xia Yang [a], Yi Xu [a,*], Bo Zhang [a,b,*]

[a] The Joint Center of Translational Precision Medicine, Department of Infections and Diseases, Guangzhou Institute of Pediatrics, Guangzhou Women and Children's Medical Center, Guangzhou, 510623, China
[b] Key Laboratory of Special Pathogens and Biosafety, Wuhan Institute of Virology, Center for Biosafety Mega-Science, Chinese Academy of Sciences, Wuhan, 430071, China
[c] University of Science and Technology of China, Department of Life Sciences and Medicine, Hefei, 230026, China
[d] Hunan Normal University, School of Medicine, Changsha, 410081, China

ARTICLE INFO

Keywords:
Hand, foot, and mouth disease (HFMD)
Enterovirus
EV-A71
High-content screening
Fangchinoline (FAN)

ABSTRACT

Hand, foot, and mouth disease (HFMD) is a common pediatric illness mainly caused by enteroviruses, which are important human pathogens. Currently, there are no available antiviral agents for the therapy of enterovirus infection. In this study, an excellent high-content antiviral screening system utilizing the EV-A71-eGFP reporter virus was developed. Using this screening system, we screened a drug library containing 1042 natural compounds to identify potential EV-A71 inhibitors. Fangchinoline (FAN), a bis-benzylisoquinoline alkaloid, exhibits potential inhibitory effects against various enteroviruses that cause HFMD, such as EV-A71, CV-A10, CV-B3 and CV-A16. Further investigations revealed that FAN targets the early stage of the enterovirus life cycle. Through the selection of FAN-resistant EV-A71 viruses, we demonstrated that the VP1 protein could be a potential target of FAN, as two mutations in VP1 (E145G and V258I) resulted in viral resistance to FAN. Our research suggests that FAN is an efficient inhibitor of EV-A71 and has the potential to be a broad-spectrum antiviral drug against human enteroviruses.

1. Introduction

Hand, foot, and mouth disease (HFMD) is a common pediatric illness caused by 20 types of enteroviruses. Most of the cases recover spontaneously within approximately one week, but severe HFMD can develop rapidly, leading to significant neurological symptom or even death. This condition has become a serious public health concern worldwide, particularly in the Asia-Pacific region (Bian et al., 2019). According to epidemiological data from the past decade, group A enterovirus (EV)-A71, coxsackievirus (CV)-A16, CV-A6, CV-A10 and group B CV-B3 and CV-B5 virus are the main pathogens responsible for HFMD (Wang et al., 2022), severe viral myocarditis and aseptic meningitis (Saguil et al., 2019; Zhang X. et al., 2022; Sharma et al., 2023). Although three inactivated EV-A71 vaccines have been available to combat HFMD (Bello and Roshorm, 2022; Kinobe et al., 2022), persistent epidemics and cross-infections continue to pose huge threats to public health. Currently, there are no effective antiviral drugs available against enteroviruses, making the development of antiviral agents urgent to control enterovirus infection.

Enteroviruses are small, nonenveloped, single-positive-strand RNA viruses with icosahedral capsids. The genomic RNA is approximately ~7.5 kb in length and contains an open reading frame (ORF) flanked by the 5′ untranslated region (5′ UTR) and 3′ UTR. The ORF encodes a single large polyprotein that is autocatalytically processed into four structural (VP1 to VP4) and seven nonstructural (2A to 2C, and 3A to 3D) proteins (Kinobe et al., 2022). The viral replication cycle of enterovirus involves several critical steps, including virus adsorption, uncoating, protein translation, polyprotein processing, genome RNA replication, virus assembly and release. Compounds that can inhibit any stage of the viral replication cycle may have potential antiviral effect.

Traditional antiviral screening techniques based on plaque or cytopathic effect (CPE) reduction assay and quantitative reverse transcription

* Corresponding authors.
E-mail addresses: xuyi70@163.com (Y. Xu), zhangbo@wh.iov.cn (B. Zhang).
[1] Qiu-Yan Zhang and Jia-Qi Li contributed equally to this work.

https://doi.org/10.1016/j.virs.2024.02.006
Received 5 July 2023; Accepted 26 February 2024
Available online 5 March 2024

polymerase chain reaction (qRT-PCR) (Bajaber and Ramanathan, 2021) are time-consuming, inconvenient and have low throughput. For enteroviruses, several high-throughput antiviral screening systems based on different strategies have been developed, including luciferase-based 3C protein biosensor system (Zhang Y. et al., 2017), fluorescence resonance energy transfer (FRET)-based biosensor detection system (Lu et al., 2017), and pseudovirus screening system carrying reporter gene (Arita et al., 2008). However, these tools are unable to target the entire viral replication process, which may result in missing the potential antiviral hits during screening. The development of reporter virus has provided a convenient platform for establishing the high-throughput system to screen antiviral drugs that target the complete viral life cycle (Ulferts et al., 2016; Zhang Z. et al., 2017), which could lead to the discovery of more promising drugs.

In the present study, we successfully developed a high-content antiviral screening system (a kind of high-throughput system utilizing high-content imaging technique) based on the EV-A71-eGFP reporter virus (Shang et al., 2013). Among 1042 natural compounds, we identified fangchinoline (FAN), an alkaloid derived from Chinese herbal medicine, as a potential broad-spectrum inhibitor of enteroviruses using this high-content system. Our findings indicate that FAN exhibits activity during the early infection stage of EV-A71 and other enteroviruses. Additionally, the selection of the FAN-resistant EV-A71 viruses revealed that the E145G and V258I site mutations in VP1 protein confer drug-resistance, indicating that the VP1 protein could be the antiviral target of FAN. Our research demonstrates that FAN is an efficient EV-A71 inhibitor and has the potential to be a broad-spectrum antiviral drug for human enteroviruses.

2. Materials and methods

2.1. Cells, viruses, compounds, and antibodies

Vero (African green monkey kidney) cells were cultured in Dulbecco's modified Eagle's medium (DMEM) supplemented with 10% fetal bovine serum (FBS), 100 units/mL penicillin, and 100 μg/mL streptomycin and incubated in 5% CO_2 at 37 °C. Wild-type (WT) EV-A71 (GenBank No: JX678881.1) and EV-A71-eGFP reporter viruses were prepared from the infectious cDNA clone (Shang et al., 2013) and stored as aliquots at −80 °C. CV-A10 and CV-B3 viruses were kindly provided by Prof. Cheng-Feng Qin, Academy of Military Medical Sciences. CV-A16-119 and CV-A16-24 (GenBank No: KC117318.1 and KC117317.1) viruses were prepared from the infectious cDNA clones (Deng et al., 2015). EV-A71-eGFP reporter viruses were used for the development of high-content antiviral screening system and selection of natural compounds library. WT EV-A71 viruses were used for antiviral activity assays and selection of resistant viruses. The natural compound library was purchased from Weikeqi Biotech (Sichuan, China). The rabbit anti-VP1 protein antibody was prepared in laboratory and mouse anti-β-actin antibody was purchased from Proteintech Company.

2.2. Plasmid production

Full-length infectious clone of EV-A71 HeN09 strain constructed previously (Shang et al., 2013) was used as skeleton to construct the VP1-mutants. The VP1-E145G, VP1-V258I and VP1-E145G + V258I mutations were introduced by fusion PCR, followed by digestion with BsiWI/AatII and ligation with T4 ligase (Thermo Scientific). The primers used for fragment amplification were shown in Supplementary Table S1. All constructs were confirmed by DNA sequencing.

2.3. RNA transcription and transfection

Full-length infectious cDNA clones of wild-type (WT) and VP1-mutants were linearized with HindIII digestion. *In vitro* transcription was conducted using MEGAscript T7 kit (Thermo Scientific) according to the manufacturer's protocols. To obtain the recombinant viruses, 1 μg WT and mutant RNA transcripts were transfected into Vero cells with 4 μL DMRIE-C reagent (Invitrogen), respectively. After 36 or 48 h, the supernatants were collected, titrated, and stored at −80 °C for subsequent experiments.

2.4. High-content screening (HCS) assay

All compounds were dissolved in dimethyl sulfoxide (DMSO) and then diluted with DMEM medium containing 2% FBS. High-content screening assay was performed in a 96-well format. NITD008, a known nucleotide analog that inhibits replication of flaviviruses and EV-A71 (Yin et al., 2009; Deng et al., 2014), was set as a positive compound. Vero cells were seeded into 96-well plates at a density of 1.0×10^4 cells per well and incubated at 37 °C with 5% CO_2 for 16 h. The cells were then infected with EV-A71-eGFP virus at the multiplicity of infection (MOI) of 0.1 in the presence of the tested drugs or DMSO. At 36 hours post-infection (hpi), the eGFP expression was observed using Perkin-Elmer, High-Content Screening System (Operetta).

2.5. Plaque assay

Virus titer and plaque morphology were determined by monolayer plaque assay. Briefly, the viruses were serially 10-fold diluted and added into 24-well plates containing confluent Vero cells (8×10^4 cells/well; plated 1 day in advance). After 1 h incubation, the supernatants were removed, and the cells were overlaid with DMEM semisolid containing 2% methylcellulose. After 4 or 5 days of incubation at 37 °C, the cells were fixed in 3.7% formaldehyde, stained with 1% crystal violet, washing under running water. The viral titer was calculated and defined as plaque forming units (PFU) per mL (PFU/mL).

2.6. In vitro antiviral assay

Vero cells were seeded in 24-well plates (8×10^4 cells per well) for antiviral assay. After one day cultivation, the cells were incubated with compound dilutions (2-fold) at different concentrations and infected with EV-A71 (MOI = 0.1). After incubation at 37 °C for 36 or 48 h, the supernatants were collected for viral titer quantification by plaque assay. The antiviral activity of compounds was defined as 50% effective concentration (EC_{50}) and calculated by GraphPad Prism software 8.0. The cells were lysed by RIPA buffer (Beyotime Biotechnology) or Trizol reagent (TaKaRa) for the measurement of viral proteins or genome RNA, respectively.

2.7. Western Blot assay

The cell lysates from antiviral assay were denatured at 95 °C for 10 min, analyzed by SDS-PAGE electrophoresis and transferred onto PVDF membrane. After being treated with skimmed milk for 2 h, PVDF membrane was successively incubated with primary antibodies against EV-A71 VP1 or β-actin and secondary horseradish peroxidase (HRP)-conjugated anti-rabbit or mouse IgG for 1 h, respectively. Finally, the PVDF membrane was incubated with a mixed substrate (Pierce ECL Western Blotting Substrate kit). The corresponding signal was detected and analyzed by the chemiluminescence system (ChemiDoc; Bio-Rad).

2.8. Quantitative reverse transcription polymerase chain reaction (qRT-PCR)

The total cellular RNA was extracted from the infected cells by Trizol reagent executing the manufacturer's protocol. qRT-PCR were performed with equal amount RNA as the templates using One Step TB Green® PrimeScript™ PLUS RT-PCR Kit (Takara, RR096A). For viral genome RNA quantification, the following primer pairs were used:

EV-A71-S1: 5′-AGATAGGGTGGCAGATGTAATTGAAAG-3′; EV-A71-R1: 5′-TAGCATTTGATGATGCTCCAATTTCAG-3′.

2.9. Cytotoxicity assays

Vero cells were seeded into 96-well plates (1×10^4 cells per well) for cytotoxicity assays. After one day cultivation, the cells were incubated with FAN of different concentrations. At 24 h post treatment, the cells were incubated with 10 μL CCK8 reagent for 1 h at 37 °C according to the manufacturer's instructions (cell counting kit 8, Bimake). The absorbance at 450 nm was measured by a multimode Microplate Reader (Varioskan Flash, Thermo Fisher). Cell activity was expressed as the percentage of the absorption value of the treated cells to the untreated cells. The 50% cytotoxic concentration (CC_{50}) was calculated by nonlinear regression using GraphPad Prism 8.0 software.

2.10. Time of addition assay

To determine which step of the viral life cycle the FAN inhibits, time-of-addition assay was conducted. Vero cells were seeded into a 24-well plate (1×10^5 cells/well) one day in advance. For all the experimental groups, the cells were infected with EV-A71 at an MOI of 10, followed by adding FAN (5 μmol/L) at various time points, including pre- (−2 h), during- (0 h) or post- (1/2/4/6/8/10 h) infection periods. The supernatants were collected for viral titer determination at 13 hpi by plaque assay. The DMSO-treatment group was set as negative control.

2.11. Disinfection test of FAN

To exclude the possibility of degermation of FAN, a disinfectant test was designed. Briefly, equal volume of viruses (10^6 PFU) and 10 μmol/L FAN or DMSO were mixed and incubated at 4 °C for 1 h. The mixtures were transferred to MicroSpin S-400 HR columns (Millipore) and centrifuged at 700×*g* for 1 min to remove the compound. The filtrates were subjected to plaque assay to determine viral titers.

2.12. Transient replicon assay

The cDNA clone of EV-A71 replicon carrying a renilla luciferase (Rluc) gene with the structural gene deletion was used to detect the genome RNA translation and replication (Xi et al., 2021). The replicon RNA was electroporated into Vero cells by a GenePulser Xcell system (Bio-Rad, Hercules, CA). Briefly, 5 μg replicon RNA was added to a 4-mm cuvette containing 8×10^6 Vero cells. Three electrical pulses were conducted at 450 V and 25 μF with three seconds intervals. After recovery at room temperature for 10 min, the electroporated cells were seeded into 12-well plate (3×10^5 cells per well), and immediately treated with 10 μmol/L FAN or DMSO. At various time points post electroporation, the cells were lysed and used for luciferase activity analysis (Promega).

2.13. Generation and sequencing of FAN-resistant EV-A71 virus

FAN-resistant EV-A71 viruses were generated by passaging the EV-A71 virus in Vero cells under the selection pressure of FAN. For each round of passage, Vero cells in 35 mm dishes were infected with 10 μL of EV-A71 (derived from the previous passage, with the first round of infection at an MOI of 0.1) in the presence of 5 μmol/L FAN or 0.5% DMSO (negative control). Three independent selections with FAN were carried out in parallel, designated as A/B/C strain, respectively. For each passage, viral supernatants were harvested at 48 hpi, and when the infected cells appeared obvious cytopathic effects (CPE) in the presence of FAN, passaging was completed. Resistance was assessed by comparing the alteration in virus titer between P8-WT and P8-A/B/C viruses treated with FAN at a concentration of 5 μmol/L. Total RNAs from P8-WT and P8-A/B/C infected cells were extracted for RT-PCR assay (TaKaRa). Four fragments that covered the full-length of genome were amplified and the gel-purified RT-PCR products were subjected to DNA sequencing. Primers used for RT-PCR and sequencing were shown in Supplementary Table S1.

2.14. Statistical analysis

Statistical analyses were performed using GraphPad Prism 8 software. The EC_{50} was defined as the compound concentration required to achieve 50% reduction of maximal viral titer. The CC_{50} was defined as 50% reduction in absorption values compared to control wells. The selectivity index (SI) was calculated as $SI = CC_{50}/EC_{50}$. Statistical calculations of Z′-values were made as follows: $Z' = 1 - [(3SD \text{ of sample} + 3SD \text{ of control}) \,|\, \text{Mean of sample} - \text{Mean of control} \,|\,]$ (Li et al., 2009; Elshabrawy et al., 2014). Here, SD is the standard deviation of the luminescent signals from control or samples. Z′ values between 0.5 and 1 are considered good quality (Martins Lima et al., 2019).

3. Results

3.1. Compound library screening

To identify compounds with antiviral activity against EV-A71, we first developed the HCS system in a 96-well plate format based on EV-A71-eGFP reporter virus (Shang et al., 2013) using NITD008 as positive control. Several parameters, such as cell density, multiplicity of infection (MOI) of virus and incubation time, were optimized and Z′ values under the different experiment condition were calculated. The condition of 10,000 cells, MOI of 0.1 and incubation time of 36 h, under which Z′ value was 0.60 (data not shown), was determined as the appropriate condition for the HCS assay. Under this condition, 1042 natural compounds (10 μmol/L), which were dissolved in 0.5% DMSO (Li et al., 2018; Zhang Q.Y. et al., 2021), were screened. A "hit" for the screening assay was defined as any compound exhibiting greater than 90% inhibition of eGFP signal, and 54 hits were screened (Fig. 1A). The Z′ factor values of the screening plates were in the range of 0.52–0.88 with an average of 0.67, indicating the robust assay performance (Fig. 1B). Among them, we selected ten compounds without obvious cytotoxicity to further confirm their antiviral effect using EV-A71 WT virus by antiviral assay. As shown in Fig. 1C, except for one compound 9E3, the other nine compounds significantly inhibited EV-A71 virus, and 2B3 (fangchinoline, FAN), which showed the strongest inhibitory effect, was selected for further characterization (Fig. 2A).

3.2. Antiviral effect of FAN

To further evaluate the antiviral activity of FAN, Vero cells were treated with DMSO or FAN at different concentrations of 1.25–10 μmol/L. As shown in Fig. 2B, FAN inhibited the EV-A71 virus in a dose-dependent manner with an EC_{50} of 0.9 μmol/L. At a concentration of 10 μmol/L, FAN resulted in about 600-fold reduction in viral titers. Meanwhile, the cytotoxicity of FAN on Vero cells were determined by CCK8 assay using serially diluted FAN (0.3–40 μmol/L). The results demonstrated that the CC_{50} of FAN was 21.14 μmol/L (Fig. 2C), yielding the SI (selection index) of 23.6. Consistently, we also observed a dose-dependent reduction in viral genome copies in the virus infected cells treated with different concentrations of FAN (Fig. 2D), and the EC_{50} calculated by viral RNA reduction was 2.86 μmol/L. In addition, with the increase of FAN concentration, the expression level of VP1 protein decreased gradually (Fig. 2E). In contrast, the expression of endogenous β-actin was not affected, indicating that the inhibition of FAN on EV-A71 replication was specific (Fig. 2E). Taken together, these data confirmed that the FAN could inhibit EV-A71 infection.

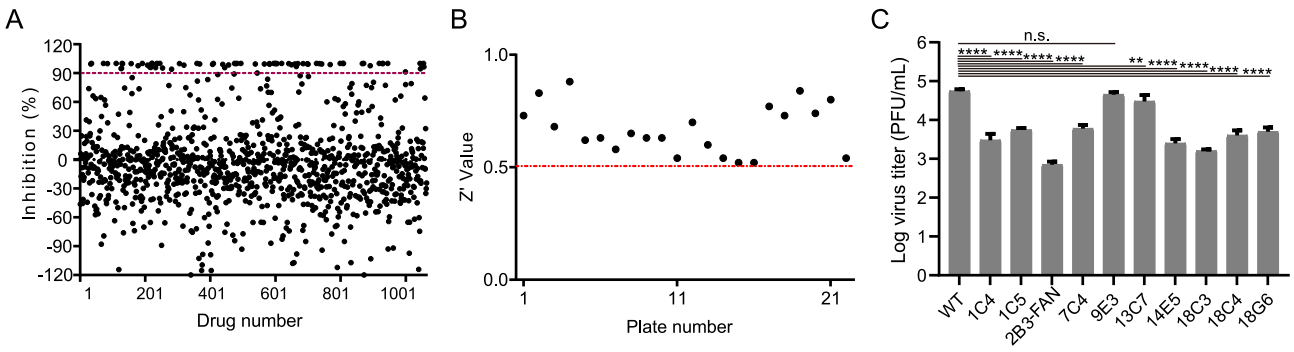

Fig. 1. High-content antiviral screening for enterovirus using EV-A71-eGFP reporter viruses. **A** Primary screening of 1042 compounds from the natural compound library at 10 μmol/L. Vero cells were infected with EV-A71-eGFP at an MOI of 0.1 in the presence of the tested drugs or DMSO in 96-well format. At 36 hours post-infection, the eGFP expression was observed using PerkinElmer, High-Content Screening System. Inhibitory effects were calculated as percent of eGFP luminescence. Hits were selected with a cutoff of 90% inhibition (dotted line). **B** The calculated Z′ values of all tested 96-well plates were shown. All values were between 0.5 and 1 and indicated the robust assay performance. **C** Identification of ten primary selected compounds for inhibition effect using EV-A71 WT virus through antiviral assay. Compounds (10 μmol/L) were added into Vero cells infected with WT virus at an MOI of 0.01 and the virus titer from the supernatants were detected at 36 hours post-infection. n.s., no significant differences. $^{**}P < 0.01$, $^{****}P < 0.0001$.

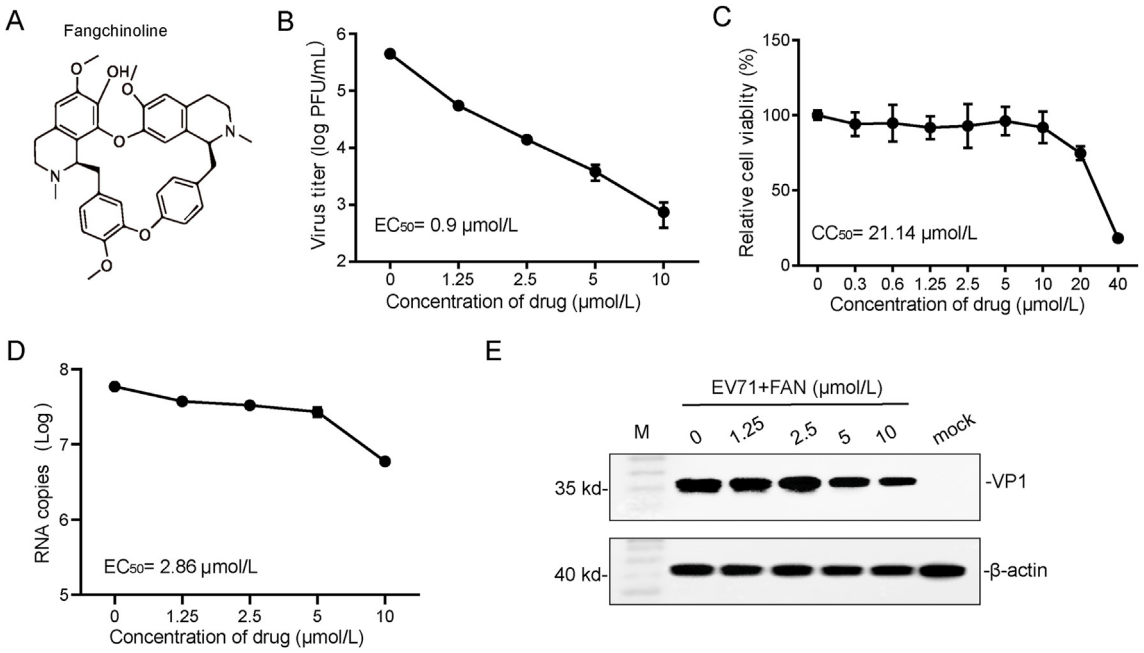

Fig. 2. Antiviral effect of fangchinoline (FAN) on EV-A71 WT virus. **A** Chemical construction of FAN. **B** Validation of FAN by antiviral assay. Vero cells were infected with EV-A71 at an MOI of 0.1 and treated with 2-fold diluted FAN. Supernatants were collected at 36 hours post-infection, and viral titers were determined by plaque assay. The data presented were obtained from two independent experiments and error bars indicate the standard deviations. **C** Validation of the cytotoxic effect of FAN on Vero cells by cytotoxicity assay with CCK8 as described in Materials and Methods. **D** Inhibition of viral RNA copies by FAN treatment. Total RNA from EV-A71 infected cells with treatment of indicated concentration of FAN was extracted and subjected to qRT-PCR assay. **E** Dose-dependent reduction of EV-A71 VP1 protein expression. The concentration of FAN in lane 1–5 was 0, 1.25, 2.5, 5 and 10 μmol/L, respectively. The value of EC_{50} and CC_{50} was analyzed using GraphPad Prism 8.0.

3.3. FAN is a broad-spectrum inhibitor of enteroviruses

To analyze whether the FAN acts on other enteroviruses, we investigated the antiviral activity of FAN against representative serotypes of various enterovirus species, such as CV-A10, CV-B3 and CV-A16, which are also significant causative agents of HFMD. FAN effectively inhibited these tested serotypes of enteroviruses, with EC_{50} values ranging from 0.86 to 1.68 μmol/L (Fig. 3A–D). In particular, the two CV-A16 strains (CV-A16-119, CV-A16-24) exhibited high sensitivity to FAN, with EC_{50} values of 0.86 and 0.93 μmol/L (Fig. 3C and D), respectively, similar to that of WT EV-A71. Those results indicate that FAN may potentially serve as a novel broad-spectrum antiviral drug against various enteroviruses.

3.4. FAN targets the early stage of enterovirus infection

To explore the potential inhibitory mechanisms, time of addition assay was conducted to determine the target stage of FAN during the viral replication cycle. As shown in Fig. 4A, Vero cells were infected with EV-A71 at an MOI of 10, and FAN (5 μmol/L) was added to the infected cells at different time points, including pre-, during- and post-infection periods. Viral titers in the culture medium were determined at 13 hpi. The results showed that the FAN exhibited the strongest inhibitory effect in maintenance groups (−2 to 13 and 0–13 h), followed by the pre- (−2 to 0 h) and during infection (0–1 h) treated groups, while it had no significantly inhibitory effect at the

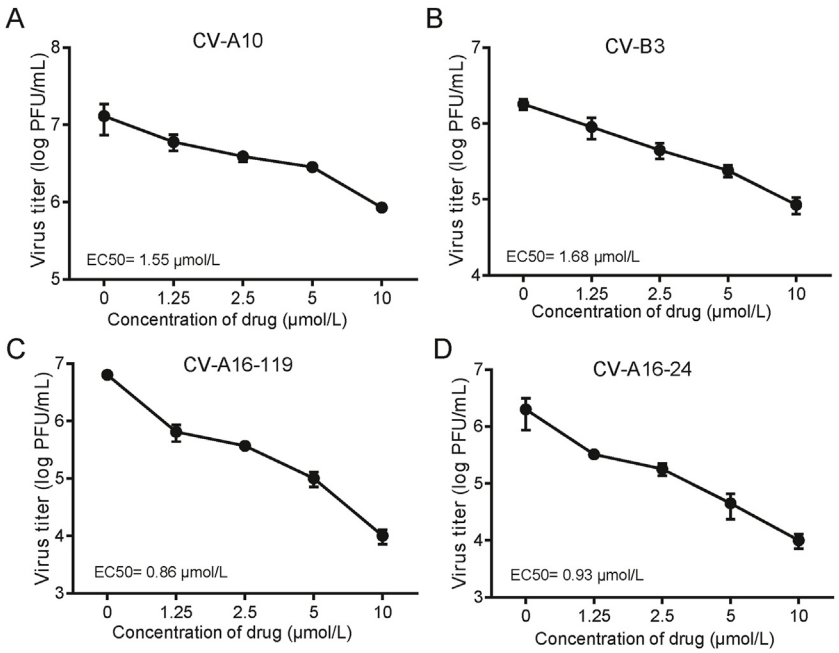

Fig. 3. Broad-spectrum anti enterovirus activity of FAN. Vero cells were infected with CV-A10 (**A**), CV-B3 (**B**), CV-A16-119 (**C**) or CV-A16-24 (**D**) at an MOI of 0.1 and treated with various concentrations of FAN. Supernatants were collected at 36 hours post-infection and viral titers were determined by plaque assay. The data shown were obtained from two independent replicates and error bars indicate the standard deviations.

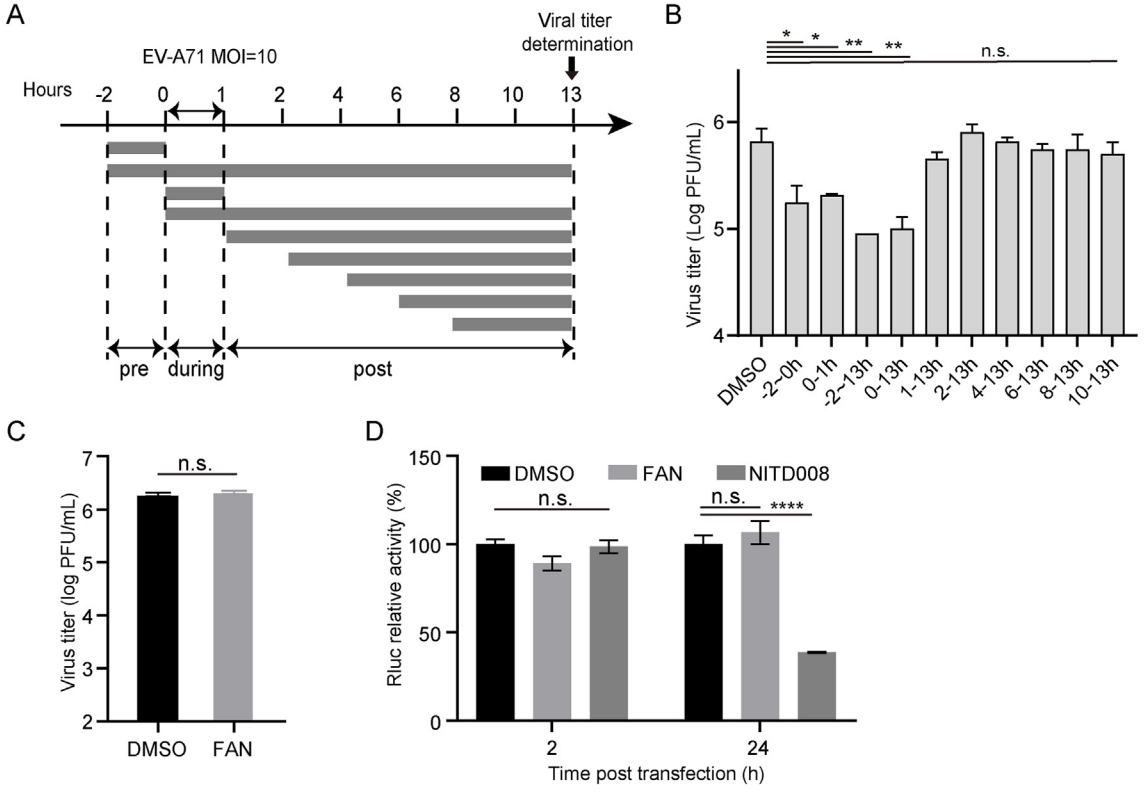

Fig. 4. Mechanism of FAN-mediated inhibition of EV-A71. **A** Schematic diagram of time of addition assay. Vero cells were infected with EV-A71 at an MOI of 10 at 37 °C for 1 h. The infected cells were washed three times with PBS. FAN (5 μmol/L) was added into Vero cells pre-, during- or post- EV-A71 infection as indicated time points. The supernatants were assayed for determination of viral titers at 13 hours post-infection. **B** Analysis of time of addition assay. Representative data from two independent experiments are shown. **C** Disinfection Test of FAN. Briefly, equal volume of viruses (10^6 PFU) and 10 μmol/L FAN or DMSO were mixed and incubated at 4 °C for 1 h. Then, the mixtures were centrifuged using the adsorption columns to remove the compound and the filtrates were subjected to plaque assay to determine viral titers. The data were shown as the mean ± SD from two independent experiments. **D** Transient replicon assay. Replicon RNA (5 μg) was electroporated into Vero cells. The electroporated cells were immediately incubated with 10 μmol/L FAN, 2 μmol/L NITD008, or 0.5% DMSO (as controls), and the luciferase activities were measured at the indicated time points. n.s., no significant differences. *$P < 0.5$, **$P < 0.01$, ****$P < 0.0001$.

post-infection stage (Fig. 4B), demonstrating that FAN acted on the early stage of infection. Similarly, we found that FAN also dramatically inhibited the entry of other enteroviruses, including CV-A10, CV-B3, CV-A16-119 and CV-A16-24 (Supplementary Fig. S1). To rule out the direct disinfection effect of FAN on virions, the equal volume of 10^6 PFU virus and 10 μmol/L FAN or DMSO were co-incubated and subjected to plaque assay to determine the viral titers. The results showed that the virus titer of EV-A71 with FAN incubation was comparable to that of DMSO-treated group (Fig. 4C), indicating that FAN has no direct viricide effect against EV-A71.

We then employed a subgenomic EV-A71 replicon in which the capsid-coding region was replaced by renilla luciferase (*Rluc*) gene to test the influence of FAN on RNA translation and replication. In transient-replicon assay, we found that Rluc activity at 2 hours post transfection (hpt) could represent the viral translation, while Rluc activity at 24 hpt represents the viral RNA replication (data not shown). Therefore, the Rluc activities at 2 and 24 hpt were measured with FAN treatment. NITD008, which had been confirmed to inhibit the RNA replication of EV-A71 (Deng et al., 2014), was used as control. As shown in Fig. 4D, treatment of FAN and NITD008 did not reduce *Rluc* signal at 2 hpt, suggesting both compounds had no effect on the RNA translation. At 24 hpt, treatment of NITD008 significantly reduced the *Rluc* activity, while treatment of FAN exhibited similar Rluc signal to that of DMSO treated control, indicating that FAN didn't inhibit the genome replication. Taken together, we concluded that FAN targeted the early stage of enterovirus infection.

3.5. Selection of FAN-resistant EV-A71

Viral resistance mutations usually indicate possible targets of compound action. Therefore, EV-A71 were serially passaged for eight rounds in the presence of 5 μmol/L FAN to select FAN-resistant viruses. Passage of EV-A71 with 0.5% DMSO was set as a control. We found that three FAN-treated passaged viruses P8-A, P8-B and P8-C showed excellent resistance to 5 μmol/L FAN, while DMSO-treated passaged EV-A71 (P8-WT) was still sensitive to FAN (Fig. 5A). In addition, there was no significant difference in plaque morphology between P8-WT and P1-WT viruses, while the resistant P8-A/B/C viruses showed smaller plaque with inconsistent sizes (Fig. 5B). The full-length genome of P8-WT and the resistant P8-A/B/C viruses was sequenced, and the mutation sites were shown in Fig. 5C. The E145G site mutation in VP1 appeared in all three resistant viruses, and other different mutations in viral structural proteins also existed but varied in P8-A/B/C viruses. The P8-WT virus only had a site mutation in 2A protein but not in structural proteins. Taken together, we obtained the FAN-resistant viruses, of which the mutations in viral structural proteins may play a role in the resistance to FAN treatment.

3.6. E145G and V258I mutations in VP1 confer viral resistance to FAN

To further validate the function of structural protein mutations in FAN resistance, we introduced VP1-E145G, VP1-V258I, and VP1-E145G + V258I (appeared in P8-B resistant virus) site mutations into the infectious clone of EV-A71. The mutant viruses were rescued as mentioned in Materials and Methods. Antiviral assay was performed using P1-WT, P8-WT, P8-B, and VP1-E145G, VP1-V258I, VP1-E145G + V258I mutant viruses with or without 5 μmol/L FAN treatment. As shown in Fig. 5D, the titer of P1-WT and P8-WT viruses were reduced dramatically about 100-fold with FAN treatment, while P8-B viruses showed excellent resistance to FAN. Notably, with the treatment of FAN, the virus titers of VP1-E145G didn't change, while the virus titers of VP1-V258I and VP1-E145G + V258I mutant decreased about 12- and 5-fold, respectively. In addition, with treatment of FAN, the virus titers of VP1-E145G and VP1-E145G + V258I viruses were comparable, suggesting that the VP1-E145G mutation determined the FAN-resistance of the virus. Notably, without FAN treatment, the virus titers of VP1-E145G + V258I were higher than that of VP1-E145G mutant, indicating that the VP1-258I mutation was able to enhance the viral replication. So, we speculated that VP1-V258I probably was an adaptive mutation and thus exhibited a certain degree of FAN-resistance. Taken together, these results demonstrate that VP1-E145G site may be the target of FAN action.

4. Discussion

HFMD has emerged as a severe health hazard in Asia-Pacific countries in recent decades. EV-A71, a kind of enteroviruses, was one of the dominant pathogens of HFMD. Although inactivated vaccines had been used in China, EV-A71 infections continue to occur annually and cause severe neurological symptoms in some cases (Zhang et al., 2014; Huang et al., 2015; Martins Lima et al., 2019; Zhang M. et al., 2021). The development of specific antiviral inhibitors is urgent and necessary work.

Natural compounds, especially medicinal herbs, and their extracts, have attracted great attention for novel therapy development. Over the past 30 years, more than 50% of the newly approved drugs were natural compounds or synthetic compounds based on or inspired by natural compounds (Newman and Cragg, 2016; Chopra and Dhingra, 2021). In this study, we screened a natural compound library based on the HCS system with EV-A71-eGFP reporter virus to find potential inhibitors against EV-A71 (Fig. 1). FAN was verified as a candidate inhibitor of EV-A71 with excellent inhibitory effect in a dose-dependent manner (Fig. 2). In addition, FAN showed significant antiviral effect against several other enteroviruses (Fig. 3), demonstrating that it is a potential broad-spectrum inhibitor against enteroviruses infection.

FAN, a bis-benzylisoquinoline alkaloid extracted from the dry roots of Stephania tetrandra S. Moore, is known to exert broad anti-cancer activity similar to tetrandrine (Liu et al., 2016). FAN can inhibit the proliferation of human breast cancer cells MCF-7 and MDA-MB-231 (Xing et al., 2013), human prostate carcinoma cells PC3 (Wang et al., 2010) and lung cancer cells A549 (Guo et al., 2015) by inducing apoptosis or autophagy. In the antiviral research, FAN demonstrates inhibitory effects against human immunodeficiency virus type 1 (HIV-1), human coronavirus OC43, and porcine epidemic diarrhea virus (PEDV) (Wan et al., 2012; Kim et al., 2019; Dong et al., 2022). It specifically targets the early stage of OC43 virus and PEDV infection (Kim et al., 2019; Dong et al., 2022). In our study, we also found that FAN acted on the early stage of EV-A71 virus infection, but not the stages of virus genome translation and replication (Fig. 4). Other bis-benzylisoquinoline alkaloids, such as tetrandrine and berbamine hydrochloride have been reported to inhibit virus entry of Ebola virus and SARS-CoV-2 by blocking endosomal calcium channels known as two pore channels (TPCs) or S protein-mediated membrane fusion, respectively (Sakurai et al., 2015; Zhang Z.R. et al. 2022). However, it remains unclear whether FAN targets the adsorption or entry stage of EV-A71 infection, which needs further exploration.

To confirm the antiviral target of FAN, we selected three FAN-resistant viruses, all of which have mutations at structural proteins (Fig. 5). The VP1-E145G and VP1-V258I mutant viruses both showed resistance to FAN, with the VP1-E145G mutant displaying particularly strong resistance (Fig. 5D). The amino acid residue 145 in VP1 affects viral fitness and pathogenesis, with different EV-A71 strains exhibiting variations at this position (145E, 81% and 145G/Q, 9%, respectively) (Kataoka et al., 2015; Kobayashi et al., 2018). Furthermore, other researchers had discovered that the E145G variation has the ability to bind the virion to the attachment receptor heparan sulfate (HS), thereby increasing the infectivity of the virus (Nishimura et al., 2013; Kobayashi et al., 2018). Those findings partially explain the resistance to FAN observed in our study.

FAN possesses diverse bioactivities and is the important component in Fangji Huangqi Tang, a traditional Chinese formula utilized in clinical settings to manage rheumatism, kidney diseases, spleen deficiency, and enhance immune function (Shan et al., 2019). Additionally, cepharanthine, sharing a similar structure with FAN, had been utilized in clinical trials for the treatment of SARS-CoV-2 infection (Fan et al., 2022). These studies further suggest the potential of FAN as a candidate for clinical applications against enteroviruses.

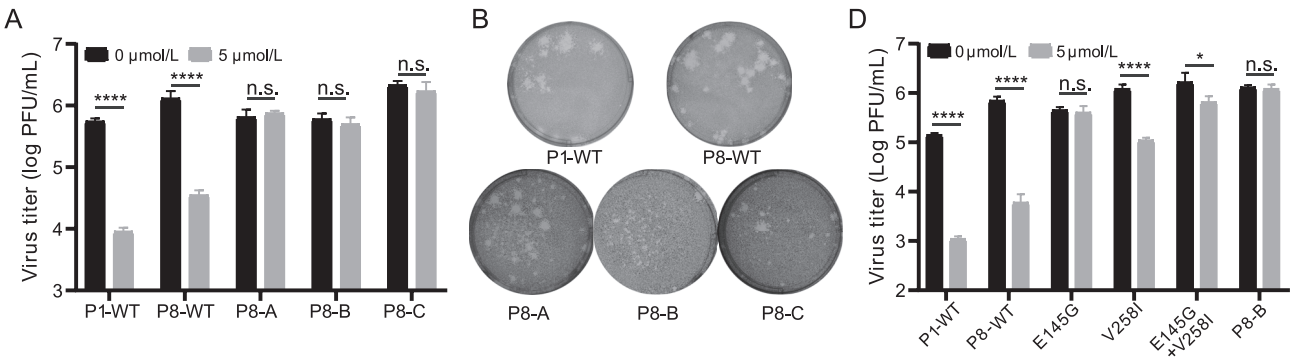

C

Virus line	VP4	VP2	VP3	VP1	VP1	2A	2B/2C	3A/3B/3C/3D
P8-A	—	—	H29Y CAC-TAC mix	E145G GAA-GGA mix	V181I GTC-ATC mix	—	—	—
P8-B	—	—	—	E145G GAA-GGA	V258I GTC-ATC mix	—	—	—
P8-C	—	A200T GCA-ACA mix	—	E145G GAA-GGA mix	V146I GTT-ATT mix	—	—	—
P8-WT	—	—	—	—	—	Y89C TAT-TGT	—	—

Fig. 5. Identification of resistant viruses and mutants. **A** Validation of the selected resistant viruses. Vero cells were infected with EV-A71 P1-WT, P8-WT or the resistant P8-A/B/C viruses at an MOI of 0.1 with or without 5 μmol/L FAN treatment. Supernatants were collected at 36 hours post-infection for viral quantification by plaque assay. **B** Plaque morphology of P1-WT, P8-WT, and resistant P8-A/B/C viruses. **C** Site mutations in passaged P8-WT or P8-A/B/C viruses. Full-length genome of P8-WT and P8-A/B/C viruses was sequenced. **D** Resistance analysis of mutant viruses by antiviral assay. Vero cells were infected with EV-A71 P1-WT, P8-WT, P8-B, and VP1-E145G, VP1-V258I, VP1-E145G + V258I mutant viruses at an MOI of 0.1 with or without FAN treatment. Supernatants were collected at 36 hours post-infection for viral quantification by plaque assay. n.s., no significant differences. $^{*}P < 0.5$, $^{****}P < 0.0001$.

5. Conclusions

Taken together, we developed an excellent high-content screening system for EV-A71, and confirmed one natural compound, FAN, as a potential broad-spectrum enteroviruses inhibitor. Our results provide the potential for the usage of FAN as a clinical therapeutic against enterovirus infection.

Data availability

All data relevant to the study are included in the article or uploaded as supplementary information.

Ethics statement

This article does not contain any studies with human or animal subjects performed by any of the authors.

Author contributions

Qiu-Yan Zhang: investigation, data curation, Funding acquisition, writing-original draft. Jia-Qi Li: investigation, methodology. Qi Li: investigation. Yang Zhang: investigation. Zhe-Rui Zhang: conceptualization, methodology. Xiao-Dan Li: conceptualization, writing-review & editing. Hong-Qing Zhang: writing-review & editing. Cheng-Lin Deng: conceptualization, methodology. Feng-Xia Yang: methodology, Supervision. Yi Xu: Funding acquisition, writing-review & editing. Bo Zhang: Conceptualization, writing-review & editing.

Conflict of interest

Prof. Bo Zhang is an editorial board member for *Virologica Sinica* and was not involved in the editorial review or the decision to publish this article. The authors declare that they have no conflict of interest.

Acknowledgments

This work was funded by Guangzhou Municipal Science and Technology Project (202102020241), the National Natural Science Foundation of China (32100110 and 32300132) and the National Key Research and Development Program of China (2021YFC2701800, 2021YFC2701801). We are grateful to Prof. Shuo Shen of Wuhan Institute of Biological Products Co. Ltd. for his helpful support during the work.

Appendix A. Supplementary data

Supplementary data to this article can be found online at https://doi.org/10.1016/j.virs.2024.02.006.

References

Arita, M., Wakita, T., Shimizu, H., 2008. Characterization of pharmacologically active compounds that inhibit poliovirus and enterovirus 71 infectivity. J. Gen. Virol. 89, 2518–2530.

Bajaber, N., Ramanathan, B., 2021. Methods in screening antiviral drugs against enterovirus 71. Methods Mol. Biol. 2296, 167–184.

Bello, A.M., Roshorm, Y.M., 2022. Recent progress and advances towards developing enterovirus 71 vaccines for effective protection against human hand, foot and mouth disease (HFMD). Biologicals 79, 1–9.

Bian, L., Gao, F., Mao, Q., Sun, S., Wu, X., Liu, S., Yang, X., Liang, Z., 2019. Hand, foot, and mouth disease associated with coxsackievirus A10: more serious than it seems. Expert Rev. Anti Infect. Ther. 17, 233–242.
Chopra, B., Dhingra, A.K., 2021. Natural products: a lead for drug discovery and development. Phytother 35, 4660–4702.
Deng, C., Li, X., Liu, S., Xu, L., Ye, H., Qin, C.F., Zhang, B., 2015. Development and characterization of a clinical strain of Coxsackievirus A16 and an eGFP infectious clone. Virol. Sin. 30, 269–276.
Deng, C.L., Yeo, H., Ye, H.Q., Liu, S.Q., Shang, B.D., Gong, P., Alonso, S., Shi, P.Y., Zhang, B., 2014. Inhibition of enterovirus 71 by adenosine analog NITD008. J. Virol. 88, 11915–11923.
Dong, S., Yu, R., Wang, X., Chen, B., Si, F., Zhou, J., Xie, C., Li, Z., Zhang, D., 2022. Bis-benzylisoquinoline alkaloids inhibit porcine epidemic diarrhea virus in vitro and in vivo. Viruses 14, 1231.
Elshabrawy, H.A., Fan, J., Haddad, C.S., Ratia, K., Broder, C.C., Caffrey, M., Prabhakar, B.S., 2014. Identification of a broad-spectrum antiviral small molecule against severe acute respiratory syndrome coronavirus and Ebola, Hendra, and Nipah viruses by using a novel high-throughput screening assay. J. Virol. 88, 4353–4365.
Fan, H., He, S.T., Han, P., Hong, B., Liu, K., Li, M., Wang, S., Tong, Y., 2022. Cepharanthine: a promising old drug against SARS-CoV-2. Adv. Biol. (Weinh) 6, e2200148.
Guo, B., Su, J., Zhang, T., Wang, K., Li, X., 2015. Fangchinoline as a kinase inhibitor targets FAK and suppresses FAK-mediated signaling pathway in A549. J. Drug Target. 23, 266–274.
Huang, Y., Zhou, Y., Lu, H., Yang, H., Feng, Q., Dai, Y., Chen, L., Yu, S., Yao, X., Zhang, H., Jiang, M., Wang, Y., Han, N., Hu, G., He, Y., 2015. Characterization of severe hand, foot, and mouth disease in Shenzhen, China, 2009-2013. J. Med. Virol. 87, 1471–1479.
Kataoka, C., Suzuki, T., Kotani, O., Iwata-Yoshikawa, N., Nagata, N., Ami, Y., Wakita, T., Nishimura, Y., Shimizu, H., 2015. The role of VP1 amino acid residue 145 of enterovirus 71 in viral fitness and pathogenesis in a cynomolgus monkey model. PLoS Pathog. 11, e1005033.
Kim, D.E., Min, J.S., Jang, M.S., Lee, J.Y., Shin, Y.S., Song, J.H., Kim, H.R., Kim, S., Jin, Y.H., Kwon, S., 2019. Natural bis-benzylisoquinoline alkaloids-tetrandrine, fangchinoline, and cepharanthine, inhibit human coronavirus OC43 infection of MRC-5 human lung cells. Biomolecules 9, 696.
Kinobe, R., Wiyatno, A., Artika, I.M., Safari, D., 2022. Insight into the enterovirus A71: a review. Rev. Med. Virol. 32, e2361.
Kobayashi, K., Sudaka, Y., Takashino, A., Imura, A., Fujii, K., Koike, S., 2018. Amino acid variation at VP1-145 of enterovirus 71 determines attachment receptor usage and neurovirulence in human scavenger receptor B2 transgenic mice. J. Virol. 92, e00681-18.
Li, J.Q., Deng, C.L., Gu, D., Li, X., Shi, L., He, J., Zhang, Q.Y., Zhang, B., Ye, H.Q., 2018. Development of a replicon cell line-based high throughput antiviral assay for screening inhibitors of Zika virus. Antiviral Res. 150, 148–154.
Li, Q., Maddox, C., Rasmussen, L., Hobrath, J.V., White, L.E., 2009. Assay development and high-throughput antiviral drug screening against Bluetongue virus. Antiviral Res. 83, 267–273.
Liu, T., Liu, X., Li, W., 2016. Tetrandrine, a Chinese plant-derived alkaloid, is a potential candidate for cancer chemotherapy. Oncotarget 7, 40800–40815.
Lu, W.W., Kung, F.Y., Deng, P.A., Lin, Y.C., Lin, C.W., Kung, S.H., 2017. Development of a fluorescence resonance energy transfer-based intracellular assay to identify novel enterovirus 71 antivirals. Arch. Virol. 162, 713–720.
Martins Lima, A., Bragina, M.E., Burri, O., Bortoli Chapalay, J., Costa-Fraga, F.P., Chambon, M., Fraga-Silva, R.A., Stergiopulos, N., 2019. An optimized and validated 384-well plate assay to test platelet function in a high-throughput screening format. Platelets 30, 563–571.
Newman, D.J., Cragg, G.M., 2016. Natural products as sources of new drugs from 1981 to 2014. J. Nat. Prod. 79, 629–661.
Nishimura, Y., Lee, H., Hafenstein, S., Kataoka, C., Wakita, T., Bergelson, J.M., Shimizu, H., 2013. Enterovirus 71 binding to PSGL-1 on leukocytes: VP1-145 acts as a molecular switch to control receptor interaction. PLoS Pathog. 9, e1003511.
Saguil, A., Kane, S.F., Lauters, R., Mercado, M.G., 2019. Hand-foot-and-mouth disease: rapid evidence review. Am. Fam. Physician 100, 408–414.
Sakurai, Y., Kolokoltsov, A.A., Chen, C.C., Tidwell, M.W., Bauta, W.E., Klugbauer, N., Grimm, C., Wahl-Schott, C., Biel, M., Davey, R.A., 2015. Ebola virus. Two-pore channels control Ebola virus host cell entry and are drug targets for disease treatment. Science 347, 995–998.
Shan, L., Tong, L., Hang, L., Fan, H., 2019. Fangchinoline supplementation attenuates inflammatory markers in experimental rheumatoid arthritis-induced rats. Biomed. Pharmacother. 111, 142–150.
Shang, B., Deng, C., Ye, H., Xu, W., Yuan, Z., Shi, P.Y., Zhang, B., 2013. Development and characterization of a stable eGFP enterovirus 71 for antiviral screening. Antivir. Res. 97, 198–205.
Sharma, V., Goessling, L.S., Brar, A.K., Eghtesady, P., 2023. Multiple subtypes of coxsackievirus group B can cause congenital heart disease. Birth Defects Res. 115, 171–178.
Ulferts, R., De Boer, S.M., Van Der Linden, L., Bauer, L., Lyoo, H.R., Mate, M.J., Lichiere, J., Canard, B., Lelieveld, D., Omta, W., Egan, D., Coutard, B., Van Kuppeveld, F.J., 2016. Screening of a library of FDA-approved drugs identifies several enterovirus replication inhibitors that target viral protein 2C. Antimicrob. Agents Chemother. 60, 2627–2638.
Wan, Z., Lu, Y., Liao, Q., Wu, Y., Chen, X., 2012. Fangchinoline inhibits human immunodeficiency virus type 1 replication by interfering with gp160 proteolytic processing. PLoS One 7, e39225.
Wang, C.D., Huang, J.G., Gao, X., Li, Y., Zhou, S.Y., Yan, X., Zou, A., Chang, J.L., Wang, Y.S., Yang, G.X., He, G.Y., 2010. Fangchinoline induced G1/S arrest by modulating expression of p27, PCNA, and cyclin D in human prostate carcinoma cancer PC3 cells and tumor xenograft. Biosci. Biotechnol. Biochem. 74, 488–493.
Wang, J., Liu, J., Fang, F., Wu, J., Ji, T., Yang, Y., Liu, L., Li, C., Zhang, W., Zhang, X., Teng, Z., 2022. Genomic surveillance of coxsackievirus A10 reveals genetic features and recent appearance of genogroup D in Shanghai, China, 2016-2020. Virol. Sin. 37, 177–186.
Xi, J., Ma, C., Wei, Z., Yin, B., Zhao, S., Quan, W., Yang, J., Yuan, J., Qiang, B., Ye, F., Peng, X., 2021. A single mutation in the cis-acting replication element identified within the EV-A71 2C-coding region causes defects in virus production in cell culture. Emerg. Microbes Infect. 10, 1988–1999.
Xing, Z., Zhang, Y., Zhang, X., Yang, Y., Ma, Y., Pang, D., 2013. Fangchinoline induces G1 arrest in breast cancer cells through cell-cycle regulation. Phytother. Res. 27, 1790–1794.
Yin, Z., Chen, Y.L., Schul, W., Wang, Q.Y., Gu, F., Duraiswamy, J., Kondreddi, R.R., Niyomrattanakit, P., Lakshminarayana, S.B., Goh, A., Xu, H.Y., Liu, W., Liu, B., Lim, J.Y., Ng, C.Y., Qing, M., Lim, C.C., Yip, A., Wang, G., Chan, W.L., Tan, H.P., Lin, K., Zhang, B., Zou, G., Bernard, K.A., Garrett, C., Beltz, K., Dong, M., Weaver, M., He, H., Pichota, A., Dartois, V., Keller, T.H., Shi, P.Y., 2009. An adenosine nucleoside inhibitor of dengue virus. Proc. Natl. Acad. Sci. U. S. A. 106, 20435–20439.
Zhang, M., Wang, H., Tang, J., He, Y., Xiong, T., Li, W., Qu, Y., Mu, D., 2021. Clinical characteristics of severe neonatal enterovirus infection: a systematic review. BMC Pediatr. 21, 127.
Zhang, Q., MacDonald, N.E., Smith, J.C., Cai, K., Yu, H., Li, H., Lei, C., 2014. Severe enterovirus type 71 nervous system infections in children in the Shanghai region of China: clinical manifestations and implications for prevention and care. Pediatr. Infect. Dis. J. 33, 482–487.
Zhang, Q.Y., Deng, C.L., Liu, J., Li, J.Q., Zhang, H.Q., Li, N., Zhang, Y.N., Li, X.D., Zhang, B., Xu, Y., Ye, H.Q., 2021. SARS-CoV-2 replicon for high-throughput antiviral screening. J. Gen. Virol. 102, 001583.
Zhang, X., Zhang, Y., Li, H., Liu, L., 2022. Hand-foot-and-mouth disease-associated enterovirus and the development of multivalent HFMD vaccines. Int. J. Mol. Sci. 24, 169.
Zhang, Y., Ke, X., Zheng, C., Liu, Y., Xie, L., Zheng, Z., Wang, H., 2017. Development of a luciferase-based biosensor to assess enterovirus 71 3C protease activity in living cells. Sci. Rep. 7, 10385.
Zhang, Z., Yang, E., Hu, C., Cheng, H., Chen, C.Y., Huang, D., Wang, R., Zhao, Y., Rong, L., Vignuzzi, M., Shen, H., Shen, L., Chen, Z.W., 2017. Cell-based high-throughput screening assay identifies 2',2'-difluoro-2'-deoxycytidine gemcitabine as a potential antipoliovirus agent. ACS Infect. Dis. 3, 45–53.
Zhang, Z.R., Zhang, Y.N., Zhang, H.Q., Zhang, Q.Y., Li, N., Li, Q., Deng, C.L., Zhang, B., Li, X.D., Ye, H.Q., 2022. Berbamine hydrochloride potently inhibits SARS-CoV-2 infection by blocking S protein-mediated membrane fusion. PLoS Negl. Trop. Dis. 16, e0010363.